Nanoscale

Accepted Manuscript

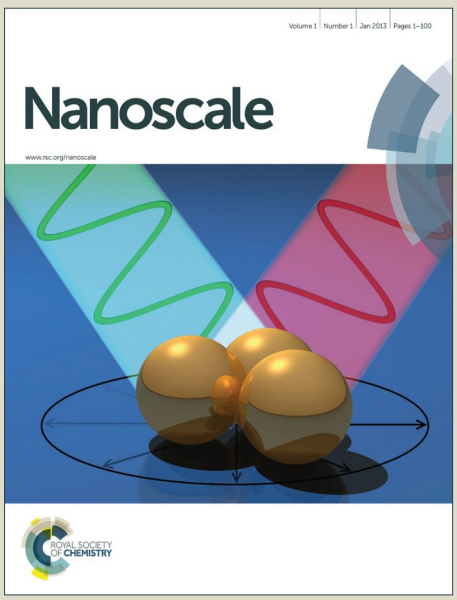

ROYAL SOCIETY OF CHEMISTRY

www.rsc.org/nanoscale

Red-green-blue laser emission from cascaded polymer membranes

Tianrui Zhai[*,1], Yonglu Wang[1], Li Chen[2], Xiaofeng Wu[1], Songtao Li[1], and Xinping Zhang[*,1]

[1]*Institute of Information Photonics Technology and College of Applied Sciences, Beijing University of Technology, Beijing 100124, China*

[2]*Department of Mathematics & Physics, North China Electric Power University, Hebei 071000, China*

**E-mail: trzhai@bjut.edu.cn and zhangxinping@bjut.edu.cn*

Abstract

Red-green-blue polymer laser emission is achieved in a free-standing membrane device consisted of three distributed feedback cavities. The polymer membrane is fabricated via interference lithography and a simple lift-off process. Multilayer structures can be assembled by cascading several polymer membranes. Thus optically pumped, simultaneous, red-green-blue laser emission is obtained from a three-layer cascaded membrane structure. This simple and low-cost fabrication technique can be used for compact, integrated laser sources.

Keywords: Red-green-blue lasers, free-standing membranes, polymer lasers

Red-green-blue (RGB) polymer lasers compatible with miniaturization and on-chip integration are highly desirable for optoelectronics.[1,2] A variety of fabrication techniques have been used to construct simple polymer laser cavities, such as nano-imprint lithography,[3-6] micromolding,[7] holographic polymerization,[8] electron beam lithography,[9] reactive ion etching,[10] and interference ablation.[11-13] However, because of the multilayer configuration, there are few methods that can be used to fabricate integrated polymer laser sources. The most promising approach for integrated sources is thin film deposition technology.[14-19] Recently, monolithic integration of multiple laser devices *via* complex procedures has been demonstrated.[20-23] Much simpler methods are needed, however, for large-scale, low-cost integration of RGB laser devices.

Here, we fabricate a RGB polymer laser from three cascaded membranes layers. Distributed feedback (DFB) lasers are fabricated using red-, green-, and blue-light-emitting polymers, respectively. After a lift-off process, the DFB polymer laser detaches from the glass substrate and forms a free-standing membrane laser, which is similar to the reported free-standing polymer laser.[23] RGB polymer lasers can then be constructed by directly cascading three polymer membranes lasers. This fabrication technique is an alternative to the integration of polymer lasers.

As noted above, the DFB cavities are fabricated with interference lithography. Specifically, the photoresist (PR, AR-P 3170) is spin-coated onto a 15×15×1 mm glass substrate at a speed of 2000 rpm, forming a 120-nm thick film, as shown in Fig. 1(a). The PR film is then exposed to an interference pattern of a continuous wave,

30-mW, 325-nm He-Cd laser (Kimmon), and developed for 3 seconds (AR 300-47 developer, Allresist) to dissolve the exposed PR film. The period Λ of the DFB cavity in Fig. 1(b) is defined by $\Lambda=\lambda/2\sin\theta$, which can be adjusted by the angle θ between the two interference beams (λ=325 nm), as shown in Fig. 2(a)–(c). The effective area of the DFB cavity is about 50 mm^2. The three light-emitting polymers Poly[9,9-dioctylfl uorenyl-2,7-diyl]–End capped with DMP (PFO, American Dye Source), poly[(9,9-dioctylfluorenyl-2,7-diyl)-alt -co-(1,4-benzo-(2,1′,3) -thiadiazole)] (F8BT, American Dye Source), and poly[2-methoxy-5-(3′,7′-dimethyloctyloxy)-1,4-phenylenevinylene] (MDMO-PPV, Sigma-Aldrich) are employed as the active materials. PFO and F8BT are dissolved in xylene at concentrations of 12.5 and 22.5 mg/ml, respectively. MDMO-PPV is dissolved in toluene at a concentration of 8.5 mg/ml. Then, three active materials are separately spin-coated onto the appropriate DFB cavity at a speed of 1000 rpm, forming a 170-nm-thick film, as shown in Fig. 1(c). The sample is then immersed in the developer for 30 min to remove the residual PR film. Automatically, the polymer membrane embedded with PR cavities lifts off from the glass substrate, forming a free-standing polymer membrane laser as shown in Fig. 1(d) and (f). To facilitate the measurement process, a 15×15×0.5 mm polyethylene terephthalate (PET) substrate with a round hole (radius=8 mm) in the center is used as a frame to support the free-standing polymer membranes. The wet polymer membrane can be easily attached to the PET frame. The flatness of the free-standing membrane can be guaranteed by the surface tension. Fig. 1(g)-(j) are photographs of blue (PFO), green (F8BT), red

(MDMO-PPV), and RGB polymer membrane lasers on PET frames, respectively. The multilayer structure can be assembled by cascading several membranes. Thus, a RGB polymer laser is formed from a three-layer cascaded membrane structure, as shown in Fig. 1(e) and (j). All film thicknesses are measured with a NanoMap-500LS contact surface profilometer.

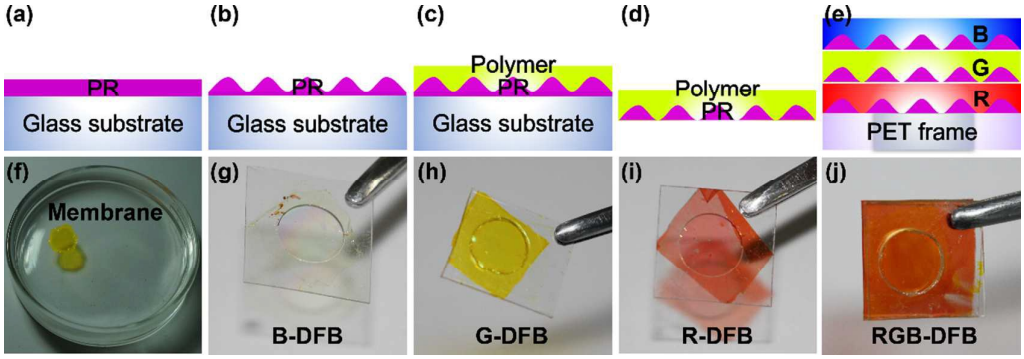

Fig. 1 (a)–(e) Schematic of RGB polymer laser fabrication. (a) A 120-nm PR film is spin-coated onto the glass substrate. (b) A PR DFB cavity is fabricated by interference lithography. (c) A light-emitting polymer is spin-coated on the DFB cavity. (d) A free-standing polymer membrane laser is obtained by lift-off from the substrate. (e) RGB polymer laser based on a three-layer cascaded membrane structure. Photographs of (f) a membrane polymer laser floating on water, (g) blue (h) green, (i) red, and (j) RGB membrane polymer lasers drying on a PET frame with a round hole in the center, respectively.

The RGB DFB cavity morphologies were characterized with scanning electron microscopy (SEM, Hitachi S-4800), as shown in Figs. 2(a)-(c). For the red, green, and blue cavities in the RGB polymer laser, Λ=285 nm, 355 nm, and 390 nm, respectively. For emission measurements, the polymer lasers are pumped by a 400-nm, 200-fs femtosecond laser at 1 kHz. The pump beam impinges on the RGB polymer laser at an angle α of 20 degrees to facilitate the actual test. Figure 2(e) is a photograph of the RGB polymer laser when the pump fluence is above the lasing threshold. Bright red,

green, and blue laser emission lines are observed, and the emission directions are determined by Bragg diffractions from the three DFB cavities. The emission from the polymer laser has a significant angular spread. Thus, the output of the surface-emitting laser should be measured in the center of the laser spots (Supplementary Section 4).

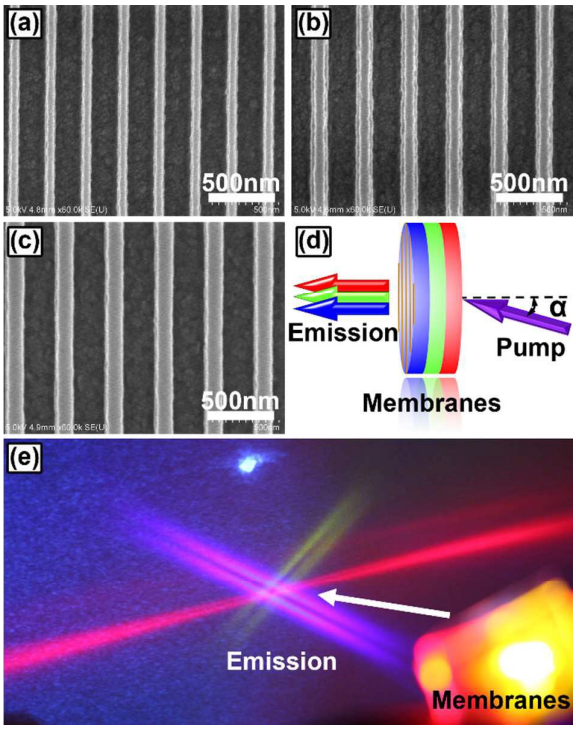

Fig. 2 SEM images of (a) blue, (b) green, and (c) red DFB PR cavities. The periods in (a)-(c) are 285 nm, 355 nm, and 390 nm, respectively. The scale bar is 500 nm. (d) Schematic of the three-layer, cascaded polymer membrane laser pumped at an angle α=20 degrees. (e) Photograph of laser spots from an operating RGB polymer laser.

The emission from the RGB polymer laser was focused into a 400-μm-diameter optical fiber using a lens and ported to a spectrometer (Maya 2000 Pro, Ocean Optics). Figure 3 plots spectra of the polymers and the RGB polymer laser emission. The

absorption and photoluminescence (PL) spectra of PFO, F8BT, and MDMO-PPV are plotted in Fig. 3(a)-(c), respectively, which are obtained directly on the single free standing membrane. The overlaps of the three absorption spectra are sufficient to allow pumping of the RGB polymer laser with a single wavelength (400 nm). However, overlaps in their absorption and PL spectra result in energy transfer between the different polymers and thus significantly affect the performance of the RGB laser.[25,26] Efficient energy transfer can be built up between two polymers. For example, part of the excitation energies in PFO and F8BT are transferred to F8BT and MDMO-PPV, respectively. Thus, the R, G, and B stacking order of the DFB cavities will affect the overall performance of the RGB laser. Here, the three DFB cavities are stacked and pumped as shown in Fig. 2(d).

An emission spectrum from a RGB polymer laser pumped by 45 μJ/cm^2 is plotted in Fig. 3(d). Three sharp laser lines at 448 nm, 566 nm, and 640 nm are shown in Fig. 3(h), with pump thresholds of 18 μJ/cm^2, 12 μJ/cm^2, and 29 μJ/cm^2, respectively. The full width at half maximum (FWHM) of the laser output is less than 1 nm, which is the resolution limit of the spectrometer. For a DFB polymer laser, the emission wavelength λ satisfies the Bragg condition $2n_{eff}\Lambda = m\lambda$, where n_{eff} is the effective refractive index of the cavity, and *m* is the diffraction order. For the surface-emitting DFB laser, feedback is provided *via* a second order diffraction process. Thus, the effective refractive indices of the R, G, and B DFB cavities are 1.57, 1.59, and 1.64, respectively. Before stacking, the pump thresholds of the blue, green, and red polymer

lasers are 27 μJ/cm^2, 14 μJ/cm^2, and 29 μJ/cm^2, respectively, as shown in Fig. 3(e)-(g).

Because of the cascaded energy transfer processes, there are small differences in the pump thresholds of the polymer laser before and after stacking. Although the pump thresholds of the individual cavities in the RGB laser increase slightly, the overall performance of the device is significantly improved *via* cascaded energy transfer (Supplementary Section 2). Thus, the largest observed threshold of the cascaded RGB laser is 29 μJ/cm^2, which is the same as that of the R component. Note that the first threshold of the cascaded RGB polymer laser (~10 μJ/cm^2) is significantly lower than that of similar polymer lasers in our previous work (~100 μJ/cm^2)[12,27], which is at the same level as that of the reported low-threshold polymer lasers[5,9]. This is attributed to the strong confinement mechanism of the free-standing membrane structure in the absence of a supporting substrate. It also implies that the polymer does not degrade during the lift-off process. So, the threshold of polymer lasers can be reduced by both employing high-efficiency light-emitting polymers[28,29] and optimizing DFB cavities[30] as shown in this work.

In Fig. 3(h), there is an intersection point among three lines of the pump slope efficiencies. This is because of the different pump slope efficiencies of the red, green, and blue DFB cavities. Thus, for the RGB polymer laser, there is an optimum operating zone indicated by the black square in Fig. 3(h), where the pump flence is around 48 μJ/cm^2. In that zone, the three emission intensities of the RGB polymer

laser are approximately equal, which may enable potential applications in new sensors.

Note that the best performance (maximum emission intensity) of the polymer laser can be obtained by adjusting the polarization of the pump beam along the grating direction of the DFB cavity, which is discussed in detail in Supplementary Section 1. Thus, a circular polarized light is employed as the pump to achieve simultaneously the best performance of three DFB cavities in this work.

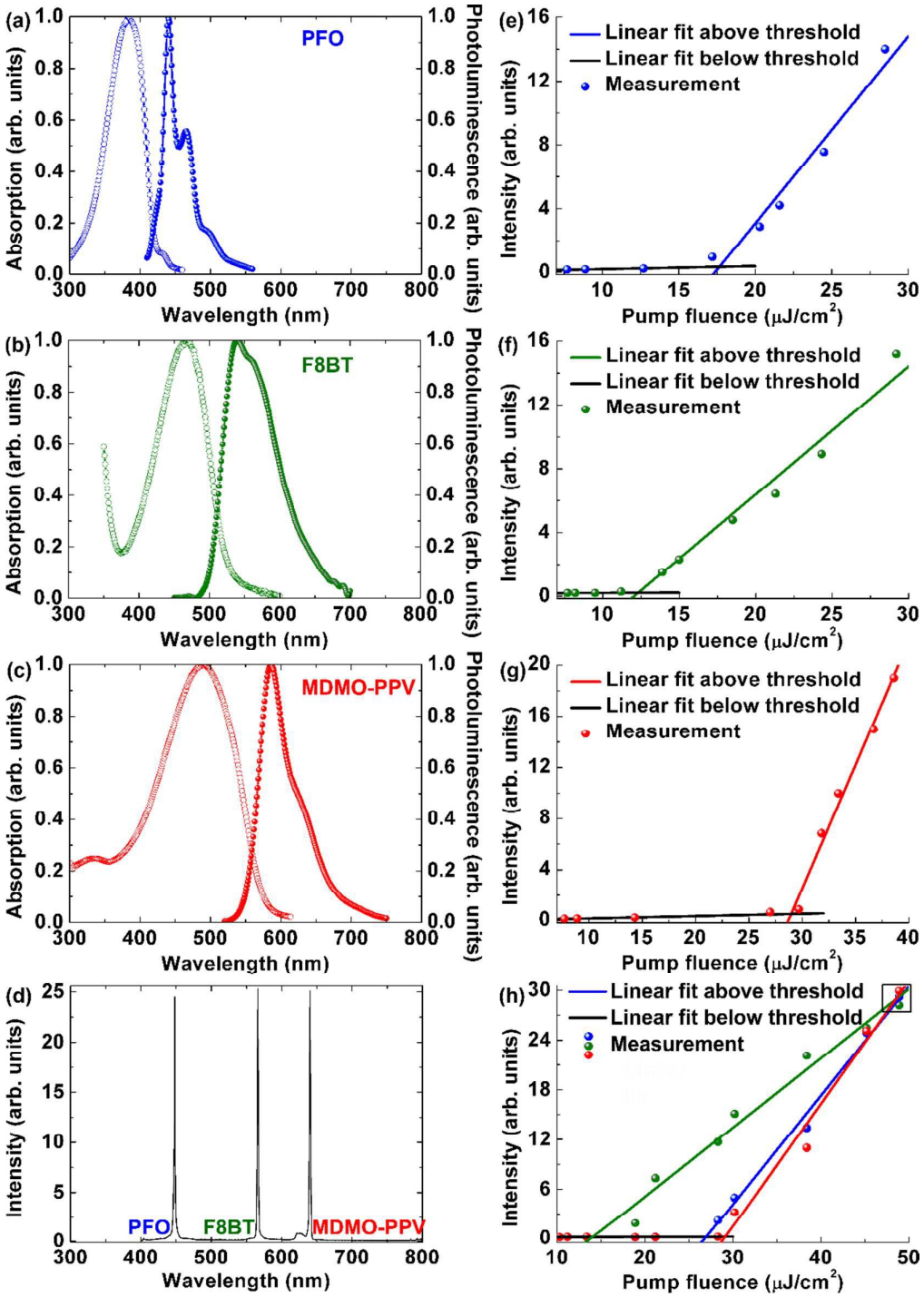

Fig. 3 Absorption and photoluminescence spectra of (a) PFO, (b) F8BT, and (c) MDMO-PPV. (d) Emission spectrum of a RGB polymer laser, pumped by 45 μJ/cm^2. The emission lines are located at 448 nm, 566 nm, and 640 nm. Output of (e) blue, (f) green, (g) red, and (h) RGB emission from the polymer laser as a function of pump fluence, indicating different lasing

thresholds. The FWHM of the laser output is <1 nm; the measurement was limited by the resolution of the spectrometer. The black square in (h) indicates the optimum operating zone of the RGB laser device.

The output intensities of three laser components change with the pump fluence as shown in Fig. 3(h), which leads to the dynamic tuning of the mixed colors. Figure 4(a) demonstrates the emission spectra of B-DFB, G-DFB, R-DFB, and RGB polymer lasers, respectively, while Fig. 4(b) presents the calculated chromaticity of these emission spectra on a CIE 1931 color diagram, which are indicated by six white circles. The two black arrows indicate the evolution of the CIE coordinates with increasing the pump intensity. The corresponding pump intensities are 30 μJ/cm^2, 40 μJ/cm^2, and 50 μJ/cm^2, respectively.

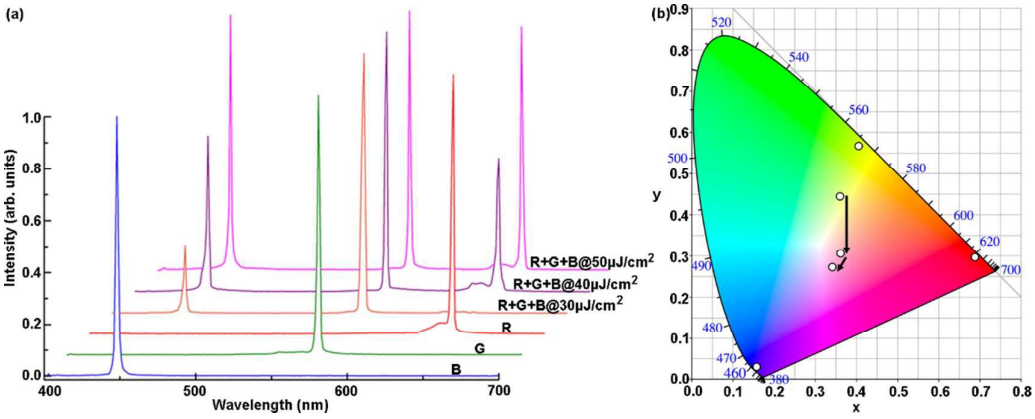

Fig. 4 (a) Emission spectra of B-DFB, G-DFB, R-DFB, and RGB polymer lasers, respectively. (b) Chromaticity of lasing spectra in (a), shown as six white circles. The two black arrows indicate the evolution of the CIE coordinates with increasing pump intensity.

In summary, we demonstrate a RGB polymer laser constructed from three cascaded membrane structures. Each polymer membrane is fabricated *via* interference lithography and a simple lift-off process. Red, green, and blue laser emissions with

low thresholds are observed for both single-membrane and multiple-membrane lasers due to the strong confinement mechanism of the membrane structure and the cascaded energy transfer process. The RGB polymer laser fabrication provides a low cost alternative to design multiple color laser devices.

Acknowledgments The authors gratefully acknowledge the financial support of the National Natural Science Foundation of China (11474014 and 11274031), the Beijing Natural Science Foundation (1132004), and the Beijing Nova Program (2012009).

References

1 F. Fan, S. Turkdogan, Z. Liu, D. Shelhammer, and C. Z. Ning, "A monolithic white laser," *Nat. Nanotechnol.* **10**, 796-803 (2015).

2 S. Furumi, "Recent advances in polymer colloidal crystal lasers," *Nanoscale* **4**, 5564-5571 (2012).

3 M. Gaal, C. Gadermaier, H. Plank, E. Moderegger, A. Pogantsch, G. Leising, and E. List, "Imprinted conjugated polymer laser," *Adv. Mater.* **15**, 1165-1167 (2003).

4 K. Yamashita, M. Arimatsu, M. Takayama, K. Oe, and H. Yanagi, "Simple fabrication technique of distributed-feedback polymer laser by direct photonanoimprint lithography," *Appl. Phys. Lett.* **92**, 243306 (2008).

5 E. Namdas, M. Tong, P. Ledochowitsch, S. Mednick, J. Yuen, D. Moses, and A. Heeger, "Low thresholds in polymer lasers on conductive substrates by distributed feedback nanoimprinting: progress toward electrically pumped plastic lasers," *Adv. Mater.* **21**, 799-802 (2009).

6 C. Ge, M. Lu, X. Jian, Y. Tan, and B. Cunningham, "Large-area organic distributed feedback laser fabricated by nanoreplica molding and horizontal

dipping," *Opt. Express* **18**, 12980-12991 (2010).

7 J. Lawrence, G. Turnbull, and I. Samuel, "Polymer laser fabricated by a simple micromolding process," *Appl. Phys. Lett.* **82**, 4023 (2003).

8 W. Huang, Z. Diao, Y. Liu, Z. Peng, C. Yang, J. Ma, and L. Xuan, "Distributed feedback polymer laser with an external feedback structure fabricated by holographic polymerization technique," *Org. Electron.* **13**, 2307-2311 (2012).

9 P. B. Deotare, T. S. Mahony, and V. Bulovic, "Ultracompact low-threshold organic laser," *ACS nano* **8**, 11080-11085 (2014).

10 P. Del Carro, A. Camposeo, R. Stabile, E. Mele, L. Persano, R. Cingolani, and D. Pisignano, "Near-infrared imprinted distributed feedback lasers," *Appl. Phys. Lett.* **89**, 201105 (2006).

11 M. Stroisch, T. Woggon, U. Lemmer, G. Bastian, G. Violakis, and S. Pissadakis, "Organic semiconductor distributed feedback laser fabricated by direct laser interference ablation," *Opt. Express* **15**, 3968-3973 (2007).

12 T. Zhai, X. Zhang, Z. Pang, and F. Dou, "Direct writing of polymer lasers using interference ablation," *Adv. Mater.* **23**, 1860-1864 (2011).

13 H. H. Fang, R. Ding, S. Y. Lu, J. Yang, X. L. Zhang, R. Yang, J. Feng, Q. D. Chen, J. F. Song, and H. B. Sun, "Distributed feedback lasers based on thiophene/phenylene co-oligomer single crystals," *Adv. Funct. Mater.* **22**, 33-38 (2012).

14 R. W. Sabnis, M. Cazeca, W. L. DiMenna, M. J. Spencer, D. J. Guerrero, and M.-S. Sheu, "Organic polymeric coatings deposited by plasma enhanced chemical vapor deposition," *J. Vac. Sci. Technol. B* **19**, 2184-2189 (2001).

15 G. B. Blanchet, C. R. Fincher, C. L. Jackson, S. I. Shah, and K. H. Gardner, "Laser ablation and the production of polymer films," *Science* **262**, 719

(1993).

16 R. Saf, M. Goriup, T. Steindl, T. E. Hamedinger, D. Sandholzer, and G. Hayn, "Thin organic films by atmospheric-pressure ion deposition," *Nat. Mater.* **3**, 323-329 (2004).

17 J. Ju, Y. Yamagata, and T. Higuchi, "Thin-Film Fabrication Method for Organic Light-Emitting Diodes Using Electrospray Deposition," *Adv. Mater.* **21**, 4343-4347 (2009).

18 C. Grivas, M. Pollnau, "Organic solid-state integrated amplifiers and lasers," *Laser Photonics Rev.* **6**, 419-462 (2012).

19 M. Wei, T. Xu, Y. Gao, G. Chen, and B. Wei, "Low threshold simultaneous multi-wavelength amplified spontaneous emission modulated by the lithium fluoride/Ag layers," *Opt. Express* **23**, 18832-18839 (2015).

20 K. Yamashita, N. Takeuchi, K. Oe, and H. Yanagi, "Simultaneous RGB lasing from a single-chip polymer device," *Opt. Lett.* **35**, 2451-2453, (2010).

21 K. Yamashita, A. Arimatsu, N. Takeuchi, M. Takayama, K. Oe, and H. Yanagi, "Multilayered solid-state organic laser for simultaneous multiwavelength oscillations," *Appl. Phys. Lett.* **93**, 233303, (2008).

22 K. Yamashita, H. Yanagi, and K. Oe, "Array of a dye-doped polymer-based microlaser with multiwavelength emission," *Opt. Lett.* **36**, 1875-1877, (2011).

23 T. Zhai, Y. Wang, L. Chen, and X. Zhang, "Direct writing of tunable multi-wavelength polymer lasers on a flexible substrate," *Nanoscale* **7**, 12312-12317, (2015).

24 Y. Chen, J. Herrnsdorf, B. Guilhabert, A. L. Kanibolotsky, A. R. Mackintosh, Y. Wang, R. A. Pethrick, E. Gu, G. A. Turnbull, P. J. Skabara, I. D. W. Samuel, N. Laurand, and M. D. Dawson, "Laser action in a surface-structured

free-standing membrane based on a p-conjugated polymer-composite," Org. Electron. 12, 62-69 (2011).

25 X. Shi, Y. Wang, Z. Wang, S. Wei, Y. Sun, D. Liu, J. Zhou, Y. Zhang, and J. Shi, "Random lasing with a high quality factor over the whole visible range based on cascade energy transfer," *Adv. Opt. Mater.* **2**, 88-93, (2014).

26 T. Xu, M. J. Wei, H. Zhang, Y. Q. Zheng, G. Chen, and B. Wei, "Concentration-dependent, simultaneous multi-wavelength amplified spontaneous emission in organic thin films using Förster resonance energy transfer," *Appl. Phys. Lett.* **107**, 123301 (2015).

27 T. Zhai, X. Zhang, and Z. Pang, "Polymer laser based on active waveguide grating structures," *Opt. Express* **19**, 6487-6492, (2011).

28 R. Xia, W.-Y. Lai, P. A. Levermore, W. Huang, and D. D. C. Bradley, "Low-threshold distributed-feedback lasers based on Pyrene-cored starburst molecules with 1,3,6,8-attached Oligo(9,9-Dialkylfluorene) arms," *Adv. Funct. Mater.* **19**, 2844-2850 (2009).

29 B. K. Yap, R. Xia, M. Campoy-Quiles, P. N. Stavrinou, and D. D. C. Bradley, "Simultaneous optimization of charge-carrier mobility and optical gain in semiconducting polymer films," *Nat. Mater.* **7**, 376-380 (2008).

30 Y. Dong, H. Zhao, J. Song, F. Gao, C. Cheng, Y. Chang, G. Du, M. Yu, and G. Lo, "Low threshold two-dimensional organic photonic crystal distributed feedback laser with hexagonal symmetry based on SiN," *Appl. Phys. Lett.* **92**, 223309 (2008).